Void Reduction in Bottom Terminated Components Using Vacuum Assisted Reflow

M. Holtzer[2], M. Barnes[1], D.W. Lee[1], D. Heller[1], T. Cucu[2], J. Fudala[3], J. Renda[3],
[1] Heller Industries, Florham Park, New Jersey (USA)
[2] Alpha Assembly Solutions, South Plainfield, New Jersey (USA)
[3] MacDermid Enthone Electronic Solutions, West Haven, Connecticut (USA)

Abstract
Pockets of gas, or voids, trapped in the solder interface between discrete power management devices and circuit assemblies are, unfortunately, excellent insulators, or barriers to thermal conductivity. This resistance to heat flow reduces the electrical efficiency of these devices, reducing battery life and expected functional life time of electronic assemblies. There is also a corresponding increase in current density (as the area for current conduction is reduced) that generates additional heat, further leading to performance degradation.

This paper will describe the results of a series of experiments performed in an in-line convection reflow oven, using a typical lead free reflow profile, with three types of bottom terminated components commonly used in power management applications. A solder paste flux and alloy with a known high level of voiding was used as the control. This solder alloy is of unique interest, despite its voiding in ambient reflow conditions, as it has shown superior resistance to failure under automotive thermal cycling conditions (-40C to +125C) and vibration.

The experimental design was comprised of two levels of vacuum (5 and 20 torr) applied at two levels of time (30 seconds and 60 seconds) while the test assemblies were at or above the liquidus temperature of the lead free solder alloy. Each 2 x 2 factorial was performed on identical printed circuit boards with four (4) different substrate surface finishes, including Immersion silver, Immersion tin, ENIG (Electroless nickel, Immersion gold) and an Organic Solder Preservative (OSP) finish used. Each condition was repeated three times and three controls with no vacuum were also processed for each surface finish. Therefore, a total of 60 component/substrate samples were processed and subsequently examined for voiding using X-ray analysis.

The results of this study indicate that the vacuum pressure, time under vacuum and the surface finish have little effect on the results when vacuum reflow is utilized. The use of a low pressure vacuum when the solder alloy is in liquidus conclusively results in a significant reduction of observable voids in each combination of surface finish and reflow process condition.

Introduction
Studies to examine void reduction in lead-free Ball Grid Array (BGA) and Bottom Terminated Components (BTC) have been reported for several years[1-5]. BGA voiding has been shown to be an easier problem to solve, using two basic techniques in a conventional reflow oven. These have shown to be effective in dozens of field application case histories in reducing BGA voiding. First, using a soak reflow profile typically reduces BGA voiding to acceptable levels versus a straight ramp profile. (Figures 1-3)

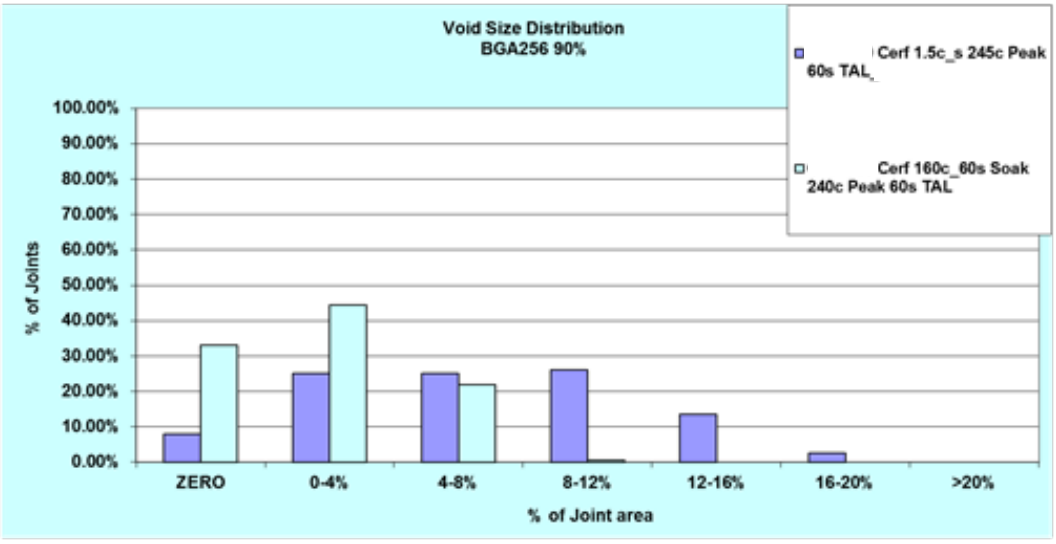

Figure 1- Effect of Reflow Profile on BGA

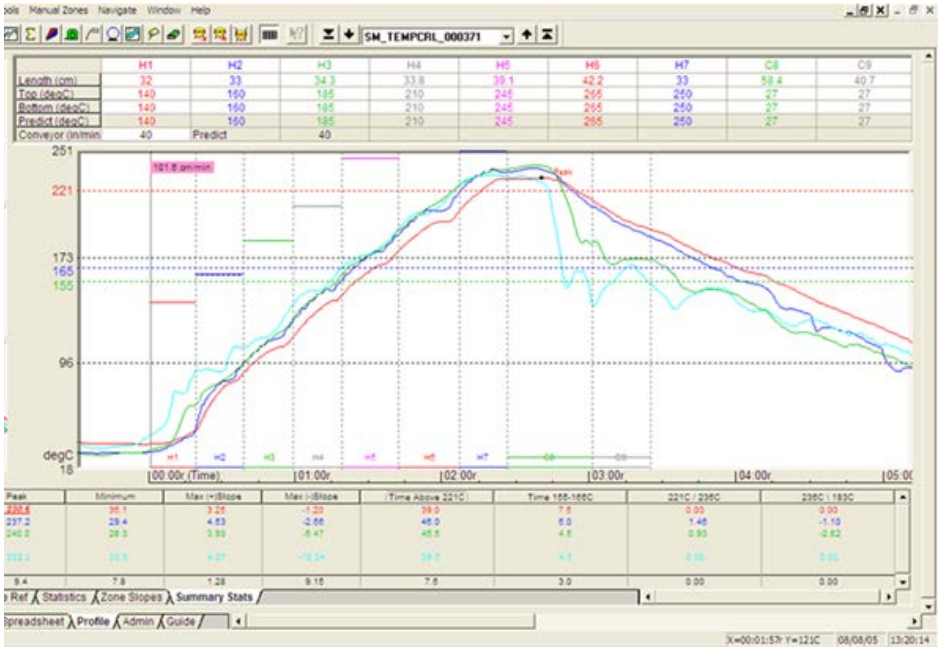

Figure 2- Straight Ramp Reflow Profile

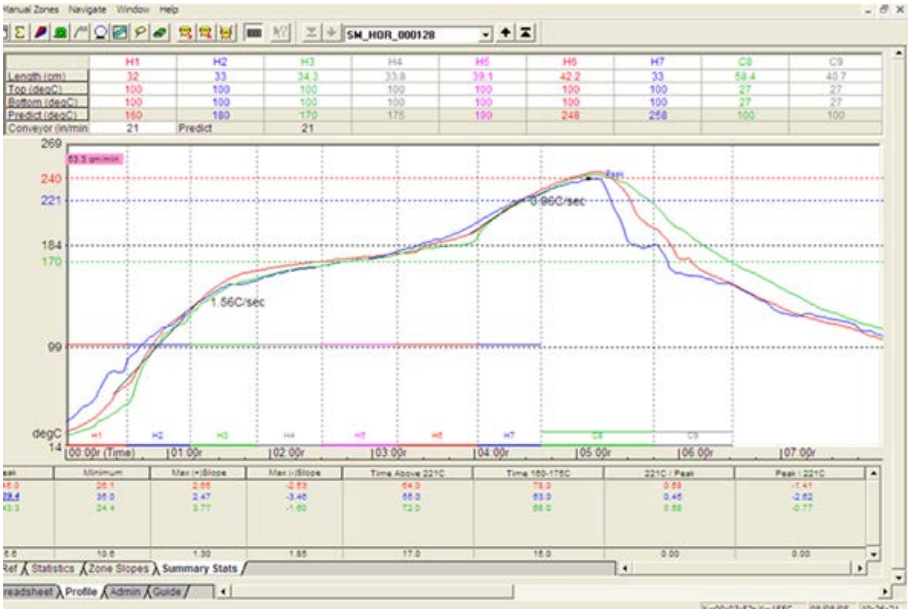

Figure 3- Soak ReflowProfile

The second reflow profile recommendation is to minimize the peak temperature since entrapped vapors will expand with increasing temperatures. X-ray videos have demonstrated this assertion is valid and does indeed promote BGA void reduction. Another effective method for reducing BGA voiding is to minimize the volume of solder paste deposited, thereby reducing the ratio of flux to metal in the BGA sphere/solder paste joint. Stencil design is the key to paste volume reduction.

BTC voiding is not as readily reduced with the same techniques. Video studies have shown that the time above liquidus can greatly reduce voids since the gas bubbles in the liquid solder are mobile and governed by Brownian motion. Longer times above liquidus allow more gas bubbles to reach the edges of the solder deposit where the bubble will disappear and not be replaced.

To enhance this bubble movement effect, the application of vacuum to the solder joint while the solder is in its molten phase has shown to be very effective in reducing BTC voids. The trapped gas bubbles expand under vacuum and are far more likely to reach the edges of the solder deposit and disappear. The pressure inside trapped gas bubbles changes according to the Young-Laplace Equation

$$P_{bubble} = P_{ambient} + 2\gamma / r$$

where γ is surface tension, r is the radius of the bubble and $P_{ambient}$ is the pressure in the vacuum reflow chamber. The reduced pressure in the bubble, $P_{bubble,}$ can then used to determine the new bubble size according to the ideal gas law.

Methodology

In this study, a known high voiding solder paste flux and powder alloy combination was used [6]. Two vacuum pressures, 5 and 20 torr were used. Two vacuum dwell times, 30 and 60 seconds were also used, making the vacuum process a 2 x 2 full factorial experimental design.

One production lot of a FR-4 test vehicle was produced, then split into 4 lots for copper surface finishing. 15 of the boards were finished with electroless nickel, immersion gold (ENIG), 15 were finished with Immersion Tin, 15 with Immersion Silver and 15 had an Organsic Surface Preservative (OSP) finish. The DOE called for 4 conditions, and 3 boards were used for each condition, leaving 3 contingency test vehicles for each surface finish.

Several spare OSP boards were used to establish the desired reflow profiles. Figure 4 shows the unpopulated company test vehicle which measured 25.4 x 13.3 x .24 cm (10 x 5.25 x .093 in.). Figure 5 shows the test vehicle populated with components. The components included MLF 100s, DPAK TO-252s, BGA 256s, and LGA 228s,

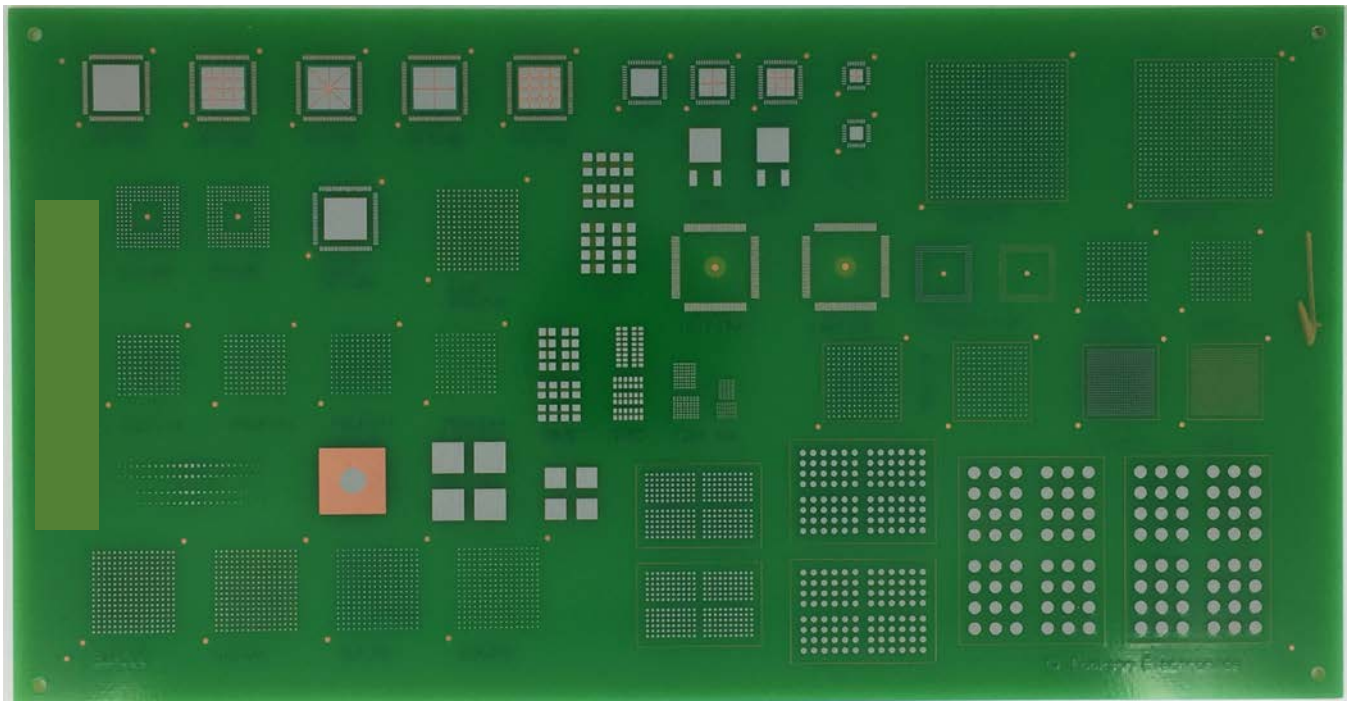

Figure 4- Unpopulated Test Vehicle

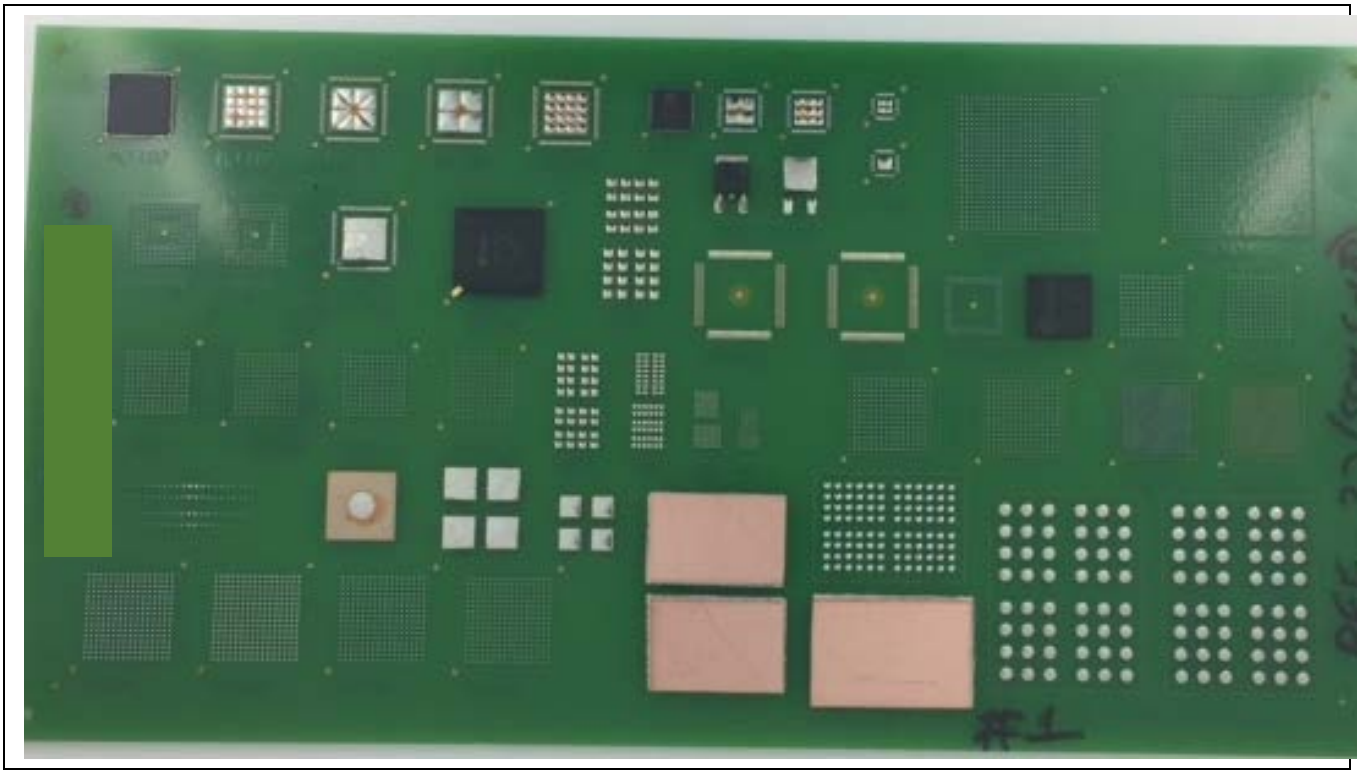

Figure 5- Populated Test Vehicle

Solder paste was printed using a 100µm thick laser cut stainless steel stencil with no coating. Components were placed, then the assemblies were fed into an air atmosphere, 8 zone convection oven with a special vacuum chamber located after convection zone 8 and before cooling zone 1. Two separate conveyors meet in this zone. As the assemblies reached the chamber, the assembly is transferred onto the second conveyor which is not moving. The vacuum chamber closes, and air is evacuated from the chamber. Figures 6 and 7 show the outline of the oven, and a close up of the vacuum chamber.

Figure 6- Eight Heat Zone Convection Oven with Vacuum Chamber in between Heat and Cooling Zones

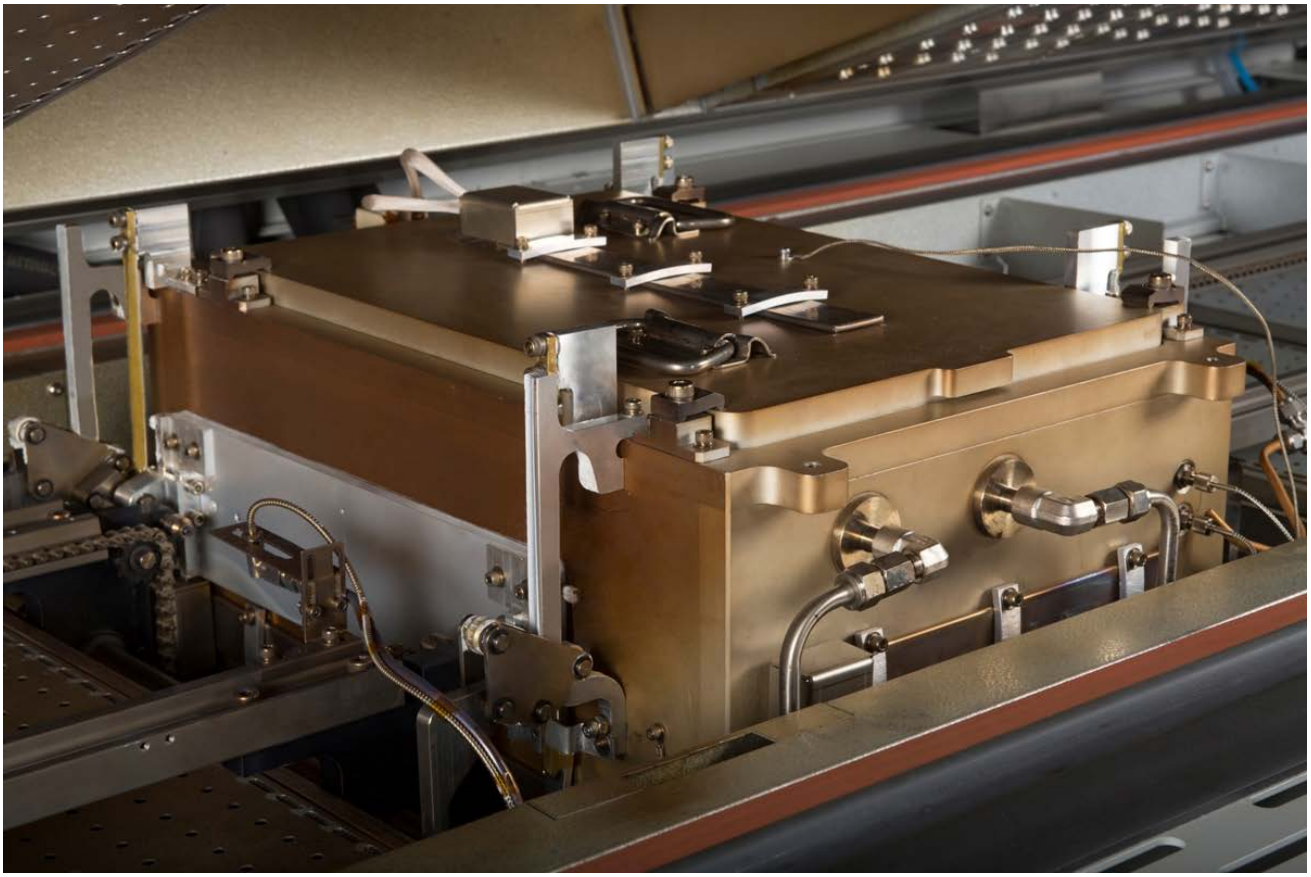

Figure 7- Vacuum Chamber Detail

Two reflow profiles were used. Both had similar 150°C to 200°C soak profiles for approximately 77 seconds, and peak temperatures measured between 240° and 245°C. Profile 1 used a 30 second dwell time in the vacuum chamber. Profile 2 used a 60 second dwell time. These reflow profiles are shown in figures 8 and 9.

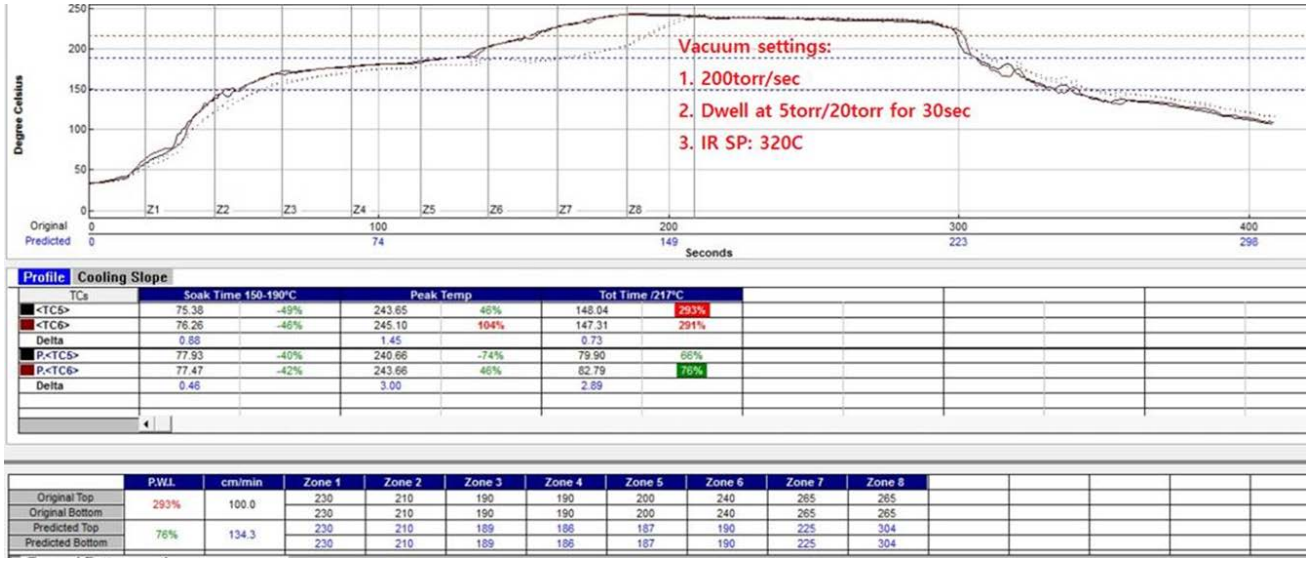

Figure 8- Reflow Profile 1; 30 seconds dwell in vacuum

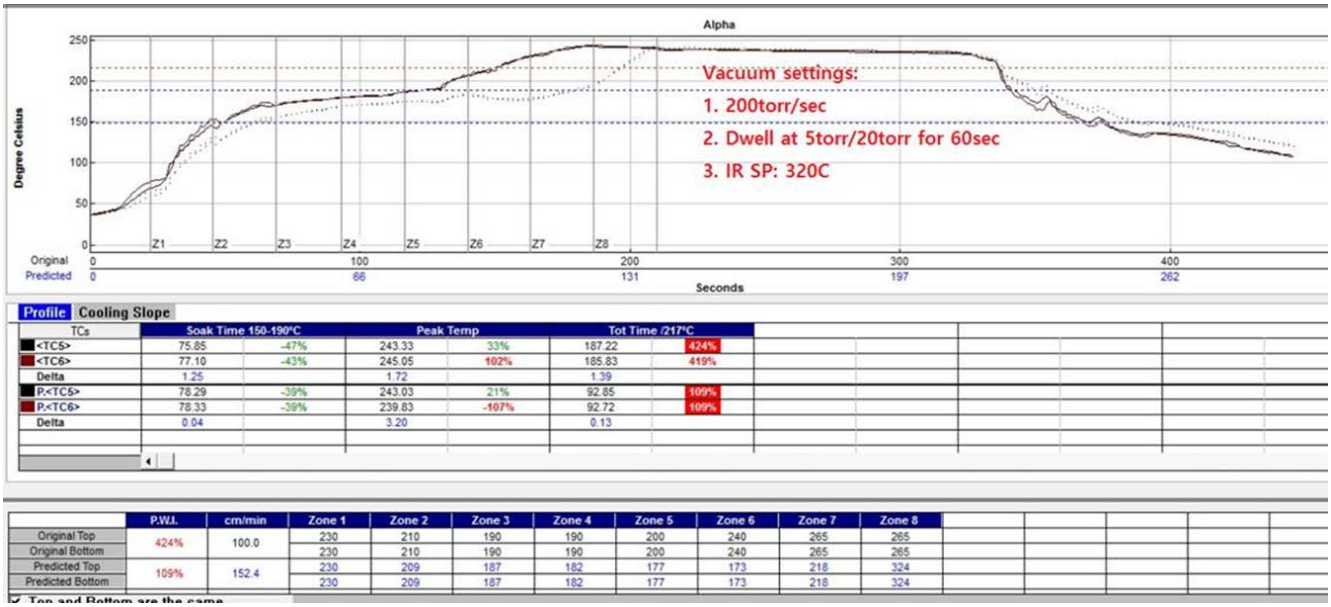

Figure 9- Reflow Profile 2; 60 seconds dwell in vacuum

In order to maintain the reflow temperature in the vacuum chamber, an IR heating element is incorporated into the upper surface of the vacuum chamber. A setpoint of 320°C is needed to maintain the peak reflow temperature depicted in Figures 8 and 9.

Experimental Procedure

In addition to the 2 x 2 x 4, pressure, dwell time and surface finish elements of the experiment, several paste print patterns were used on the MLF 100 center heat sink pad. It has been reported that by providing channels for vapor to escape, BTC voiding can be reduced [6]. For each condition 3 sets of test vehicles and components were used. There were a total of 48 assemblies, each with 3 BTCs and one BGA, resulting in a total of 28,176 solder joints. After reflow, 2D X-ray images were developed and representative images are shown in Appendix A.

Results and Discussion

Based on the results from this study indicated in Appendix A, void reduction under vacuum reflow has very little dependence on surface finish. Now that this is understood, it would be interesting to see if prior lead free reflows would have an effect on voiding, particularly with the immersion tin finish. Creation of increased Cu_6Sn_5 intermetallic at the pad surface makes this a potentially challenging substrate for lead free solder applications.

Also demonstrated in this study was that the level of vacuum (5 torr and 20 torr) had a marginal effect on the void reduction. Both levels of vacuum gave extremely low (well below 0.2% in the MLF 100 heat sink area) levels of voiding as a % of the total area of the solder joint. From this result, there appears to be no marginal return in generating a lower level of vacuum than 20 torr. Moreover, there was a lack of response for dwell time under vacuum when the solder in the assemblies is above the alloy liquidus (218°C). The 60 second dwell samples showed similar levels of void reduction when compared to the 30 second dwell time samples. Both dwell times showed excellent void reduction results so there was no room for improvement by increasing the dwell time to 60 seconds. More experiments need to be run to determine what the curves of vacuum level and vacuum dwell time versus voiding area might look like, or whether void reduction is a simple step function for both of these DOE parameters.

The most obvious conclusion of this work was that applying vacuum while the solder alloy is in the liquid phase has a significant affect on reducing BTC component voiding. The BGA 256 samples had low levels of voiding with or without vacuum. This was expected because of the long soak profile and relatively small deposits (.4mm circles, .1mm high) of the BGA packages. The effect on the larger area solder paste deposits, the heat sinks on the MLF 100 and TO-252 packages, was much more significant as can be seen in figures 10 and 11.

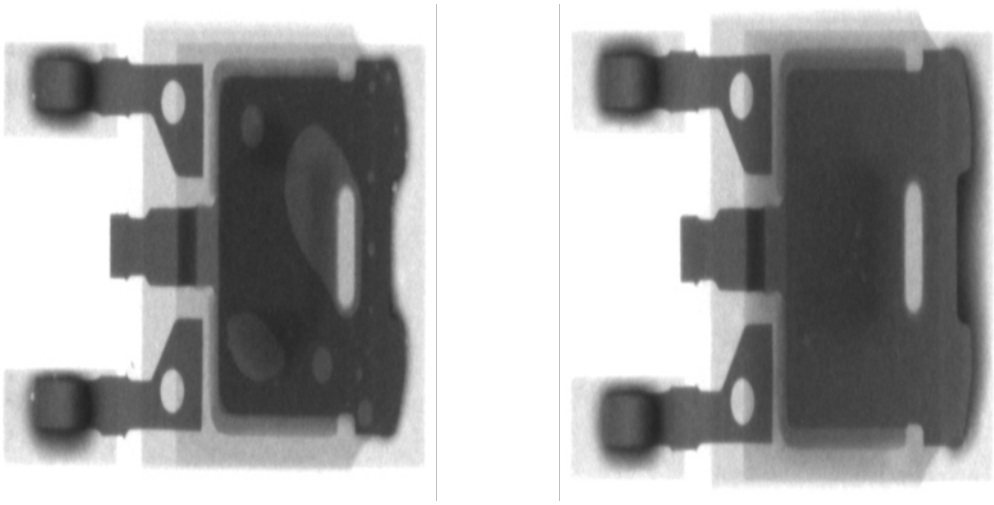

Figure 10- TO-252 Package with no vacuum (left) and 5 torr for 60 seconds vacuum (right)

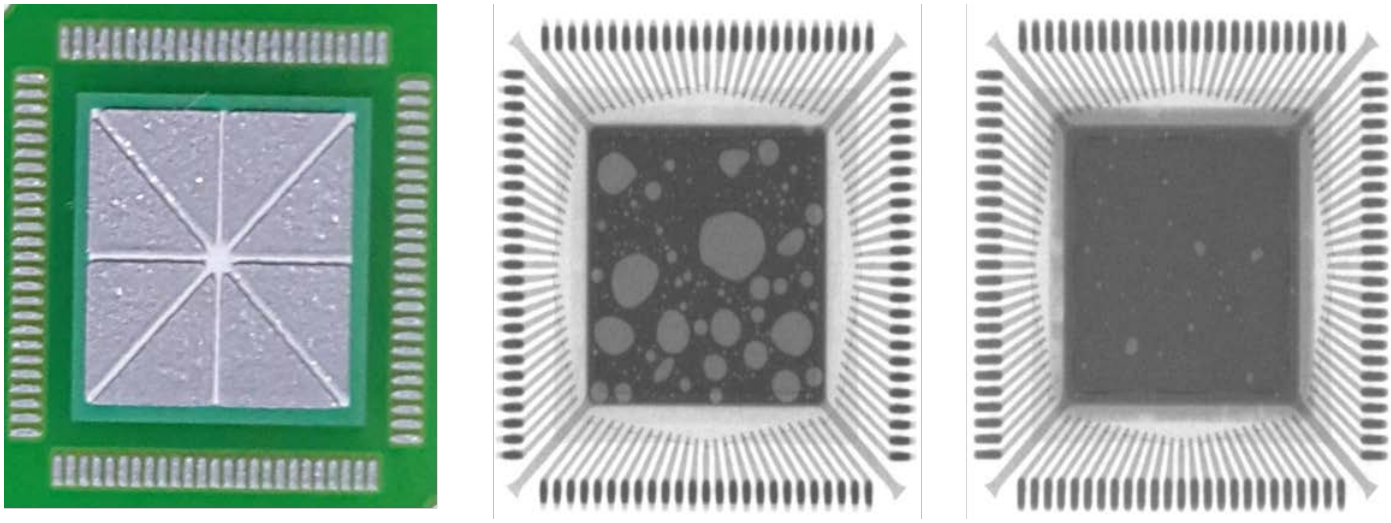

Figure 11- MLF 100 Package with no vacuum (center) and 5 torr for 60 seconds vacuum (right). Note channel pattern used (left).

Conclusions

The use of a vacuum chamber in an in-line convection reflow oven has the potential to reduce voiding significantly in large area pads designed to draw heat away from power semiconductors. This allows for more effective heat dissipation, less heat generation, longer battery life) and more reliable assemblies.

Using 20 torr of vacuum and 30 seconds of dwell time was sufficient to cause this significant reduction in voiding. Sixty second dwell in the vacuum showed no additional (significant) decrease in the level of voiding observed. Likewise, reducing the atmospheric pressure from 20 torr to 5 torr did not show a measureable improvement in void reduction. Finally, the four surface finishes used in this study all showed the same level of void reduction using the vacuum process while the solder alloy was in the molten phase.

References

1. Herron, D, Liu, Y, and Lee, N.C., Voiding Control At QFN Assembly, SMTAI, Forth Worth, TX, 2011.

2. Nguyen J., Geiger D., Shangguan D. Assembly Challenges of Bottom Terminated Components APEX, San Diego, CA, 2012.

3. Aspandiar R., "Voids in Solder Joints", SMTAI Conference Proceedings, 2006.

4. Holtzer M, Mok T.W., Methods of Reducing or Eliminating Voids in BGA and BTC Components, SMTA South Asia, 2016

5. IPC Solder Products Value Council, "The Effect of Voiding in Solder Interconnections Formed from Lead-free Solder Pastes with Alloys of Tin, Silver and Copper", White Paper, IPC.

6. Brown, S., Holtzer, M., Process Considerations in Reducing Voiding in High Reliability Lead Free Solder Joints

Appendix A:

1. QFN “MLF 100” of With Vacuum & Without Vacuum

Type 1 # without Vacuum # with Vacuum (5torr 60sec)

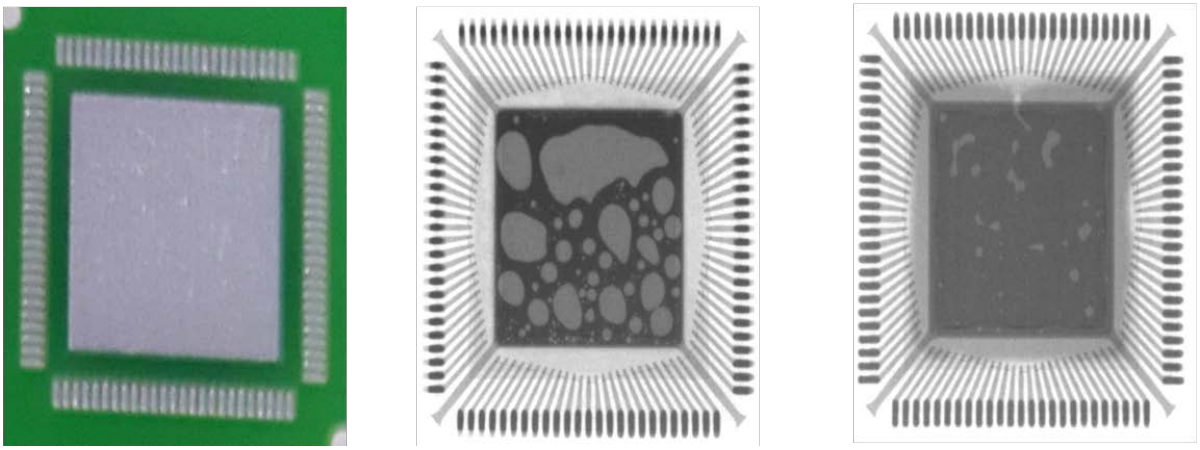

Figure 12

1. QFN “MLF 100” of With Vacuum & Without Vacuum

Type 2 # without Vacuum # with Vacuum (5torr 60sec)

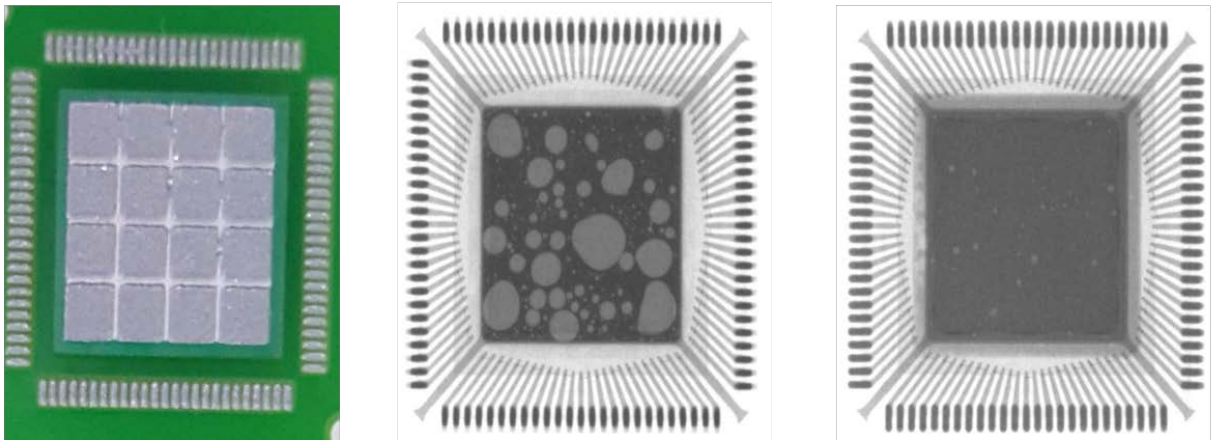

Figure 13

1. QFN “MLF 100” of With Vacuum & Without Vacuum

Type 3 # without Vacuum # with Vacuum (5torr 60sec)

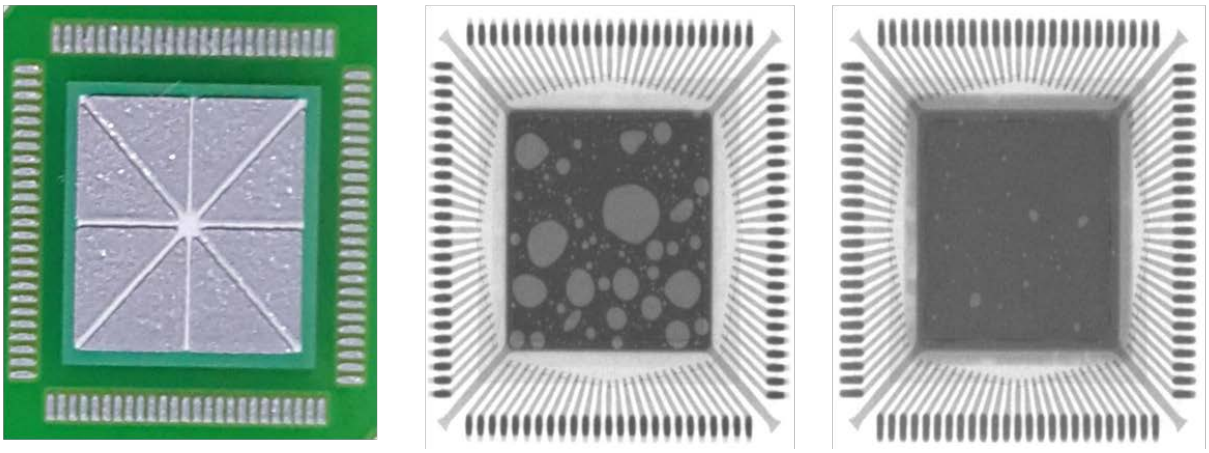

Figure 14

1. QFN “MLF 100” of With Vacuum & Without Vacuum

Type 4 # without Vacuum # with Vacuum (5torr 60sec)

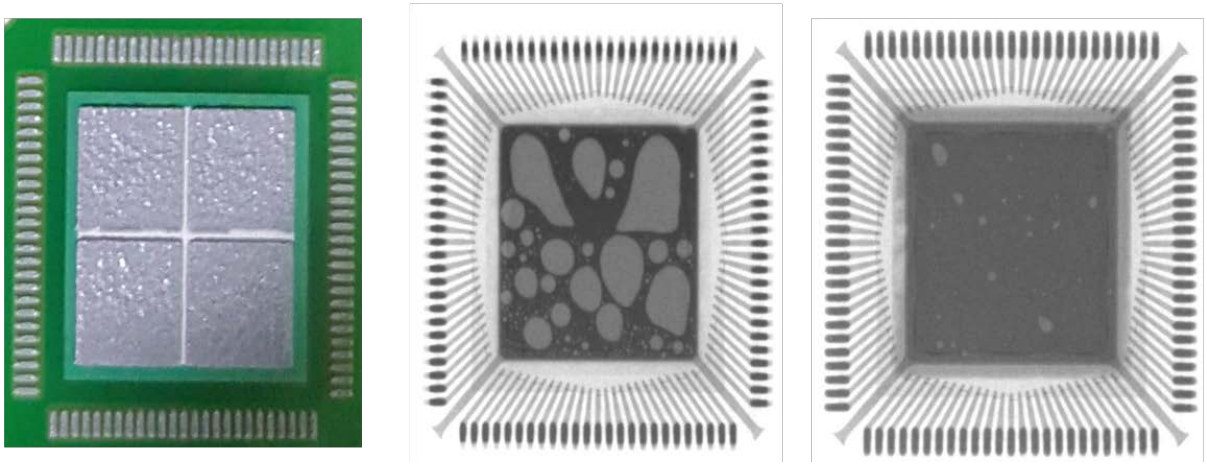

Figure 15

1. QFN “MLF 100” of With Vacuum & Without Vacuum

# Type 5	# without Vacuum	# with Vacuum (5torr 60sec)

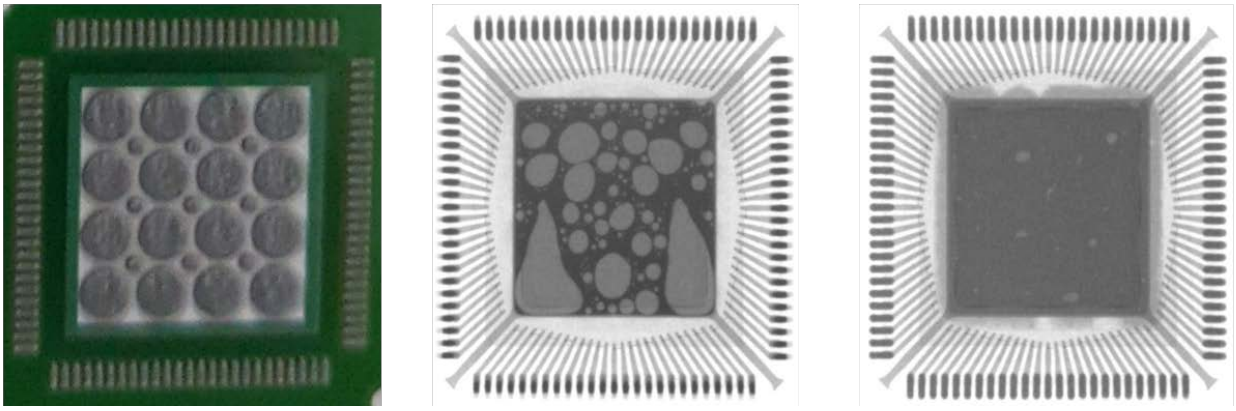

Figure 16

1. TR “TO-252” of With Vacuum & Without Vacuum

# Type	# without Vacuum	# with Vacuum (5torr 60sec)

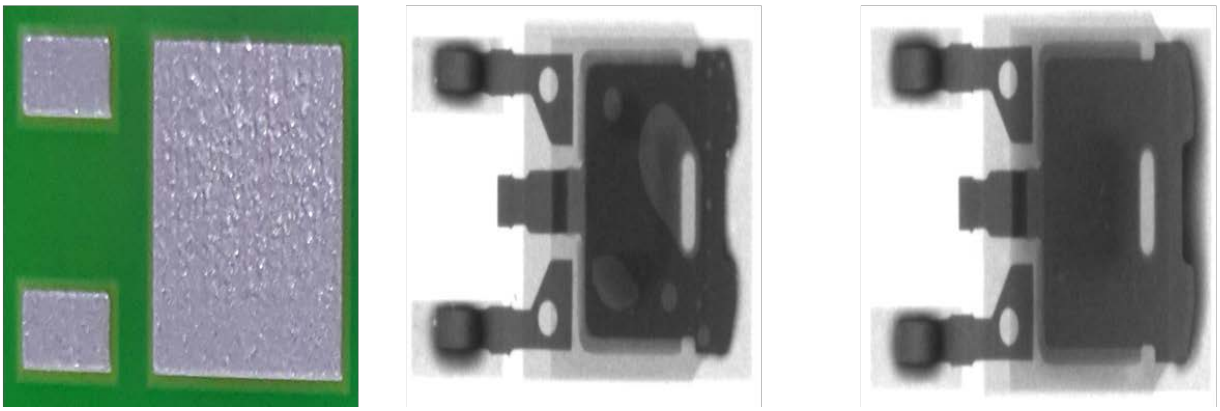

Figure 17

1. BGA “BGA 256” of With Vacuum & Without Vacuum

# Type	# without Vacuum	# with Vacuum (5torr 60sec)
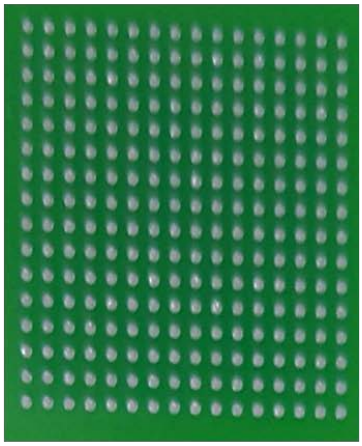	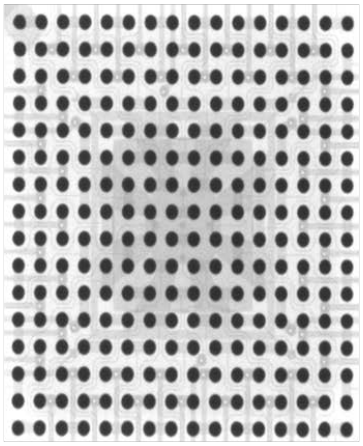	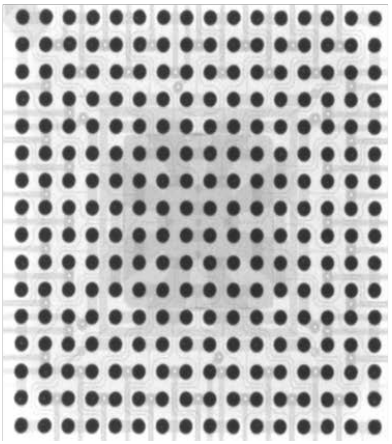

Figure 18

1. BGA “LGA 228” of With Vacuum & Without Vacuum

# Type	# without Vacuum	# with Vacuum (5torr 60sec)
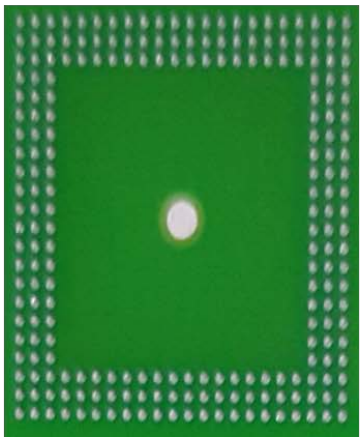	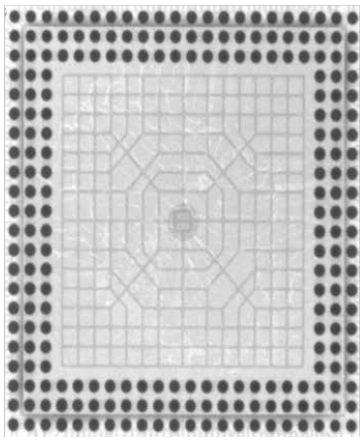	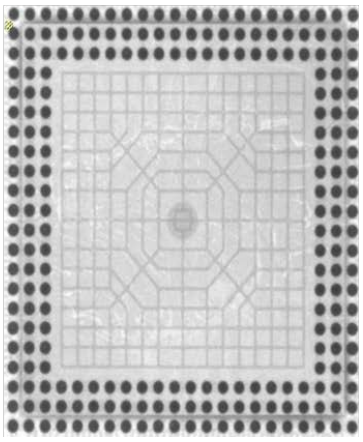

Figure 19

ENIG (5torr / 30sec)

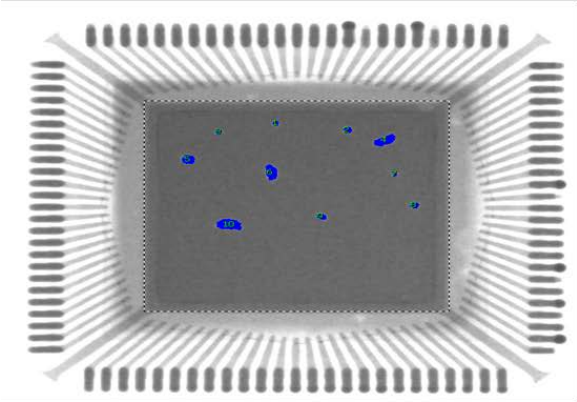

Object Count	10
Object Area	0.608
Total Area	508.7804
Total Area Ratio	0.12%
AOI Area	49.6856
AOI Area Ratio	1.22%

ENIG (5torr / 60 sec)

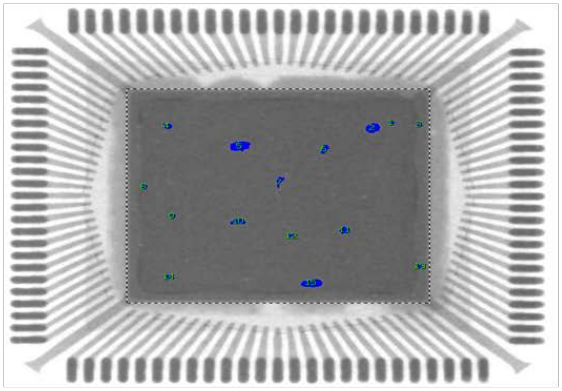

Object Count	15
Object Area	1480
Total Area	1327104
Total Area Ratio	0.11%
AOI Area	129958
AOI Area Ratio	1.14%

Figure 20

ENIG (20torr / 30sec)

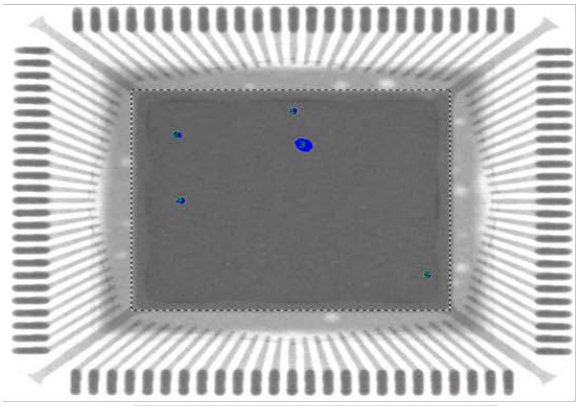

Object Count	5
Object Area	0.2059
Total Area	508.7804
Total Area Ratio	0.04%
AOI Area	48.7241
AOI Area Ratio	0.42%

ENIG (20torr / 60 sec)

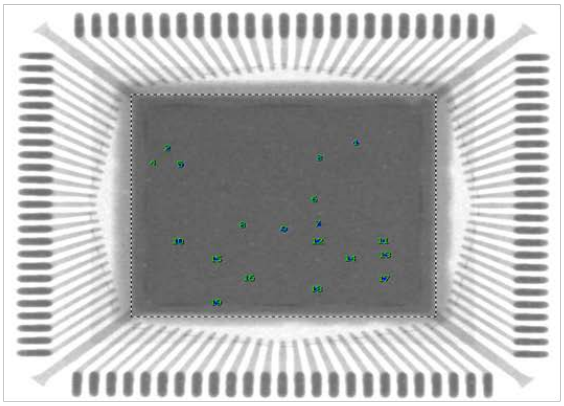

Object Count	19
Object Area	0.176
Total Area	508.7804
Total Area Ratio	0.03%
AOI Area	50.6555
AOI Area Ratio	0.35%

Figure 21

SN (5 torr / 30sec)

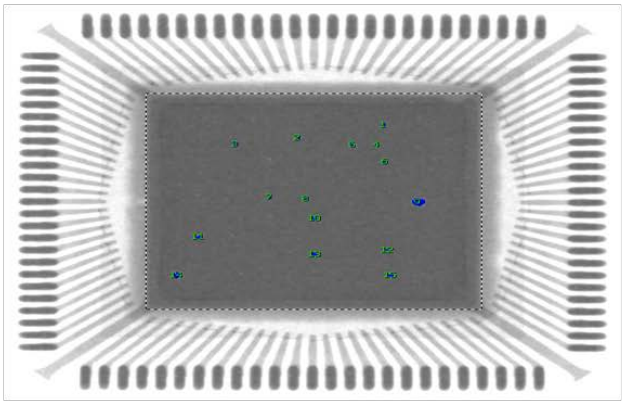

Object Count	15
Object Area	0.1649
Total Area	508.7804
Total Area Ratio	0.03%
AOI Area	50.1004
AOI Area Ratio	0.33%

SN (5 torr / 60 sec)

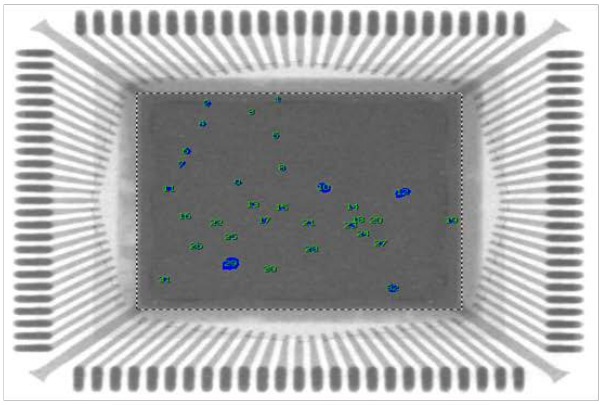

Object Count	32
Object Area	1694
Total Area	1327104
Total Area Ratio	0.13%
AOI Area	127804
AOI Area Ratio	1.33%

Figure 22

SN (20 torr / 30sec)

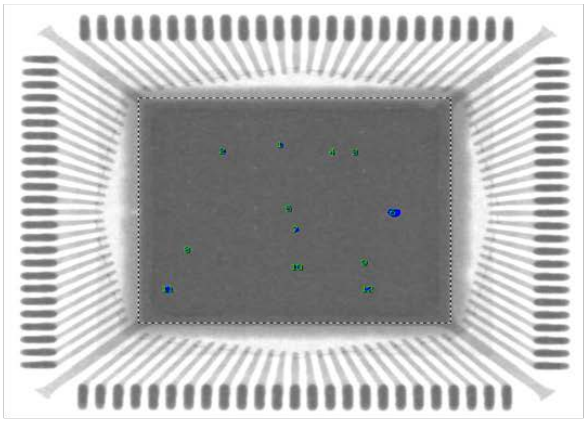

Object Count	12
Object Area	0.1779
Total Area	508.7804
Total Area Ratio	0.04%
AOI Area	49.4099
AOI Area Ratio	0.36%

SN (20 torr / 60 sec)

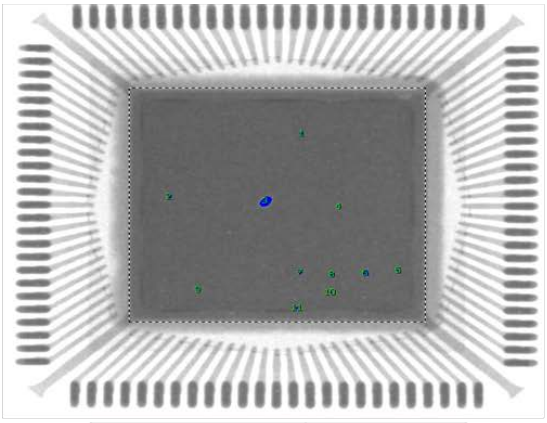

Object Count	11
Object Area	0.1365
Total Area	508.7804
Total Area Ratio	0.03%
AOI Area	50.2357
AOI Area Ratio	0.27%

Figure 23

Ag (5 torr / 30sec)

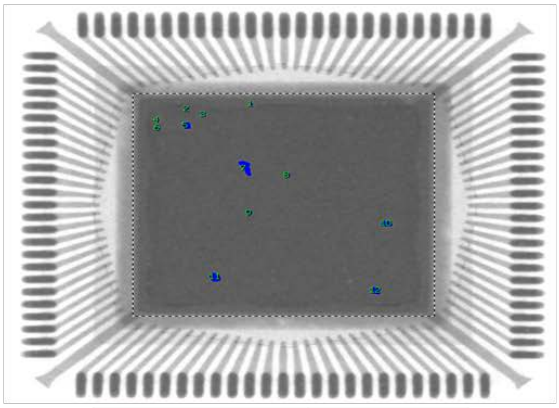

Object Count	12
Object Area	777
Total Area	1327104
Total Area Ratio	0.06%
AOI Area	132496
AOI Area Ratio	0.59%

Ag (5 torr / 60 sec)

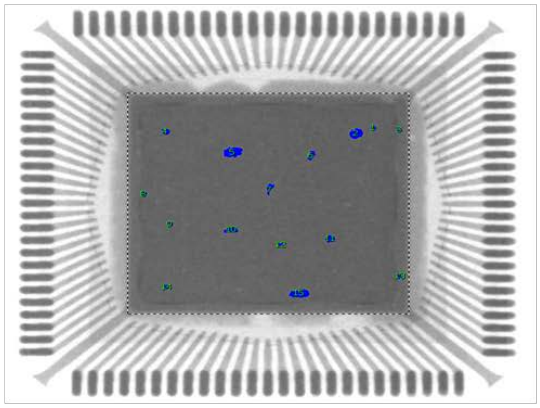

Object Count	15
Object Area	1480
Total Area	1327104
Total Area Ratio	0.11%
AOI Area	129958
AOI Area Ratio	1.14%

Figure 24

Ag (20 torr / 30sec)

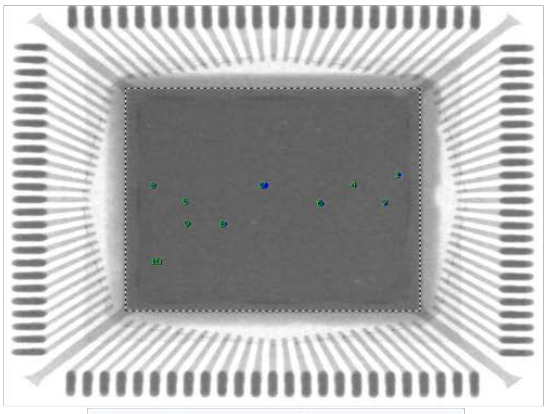

Object Count	10
Object Area	0.1158
Total Area	508.7804
Total Area Ratio	0.02%
AOI Area	48.315
AOI Area Ratio	0.24%

Ag (20 torr / 60 sec)

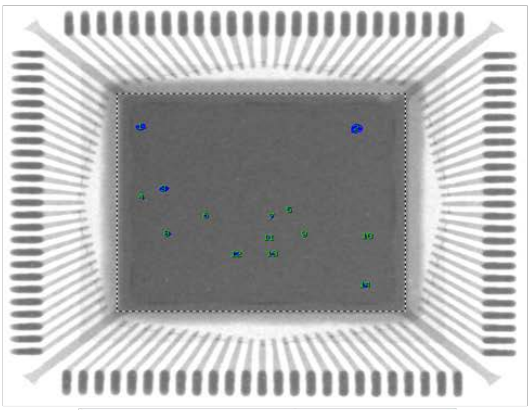

Object Count	14
Object Area	0.2339
Total Area	508.7804
Total Area Ratio	0.05%
AOI Area	49.5468
AOI Area Ratio	0.47%

Figure 25

OSP (5 torr / 30sec)

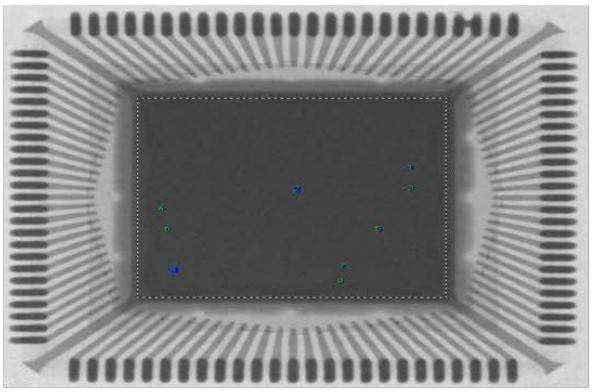

Object Count	9
Object Area	384
Total Area	1327104
Total Area Ratio	0.03%
AOI Area	150926
AOI Area Ratio	0.25%

OSP (5 torr / 60 sec)

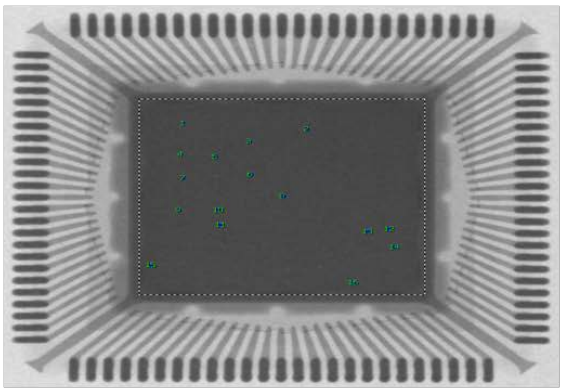

Object Count	16
Object Area	443
Total Area	1327104
Total Area Ratio	0.03%
AOI Area	145542
AOI Area Ratio	0.30%

Figure 26

EP.HT (20 torr / 30sec)

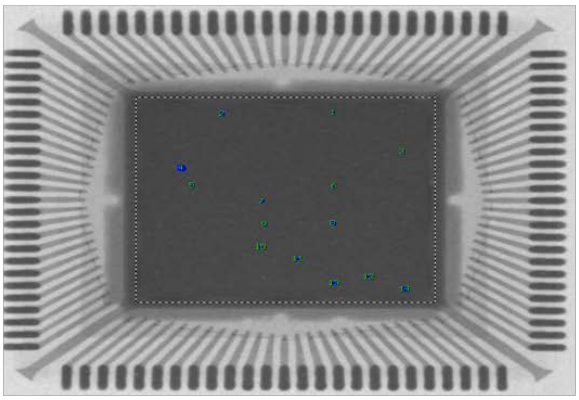

Object Count	14
Object Area	535
Total Area	1327104
Total Area Ratio	0.04%
AOI Area	147447
AOI Area Ratio	0.36%

EP.HT (20 torr / 60 sec)

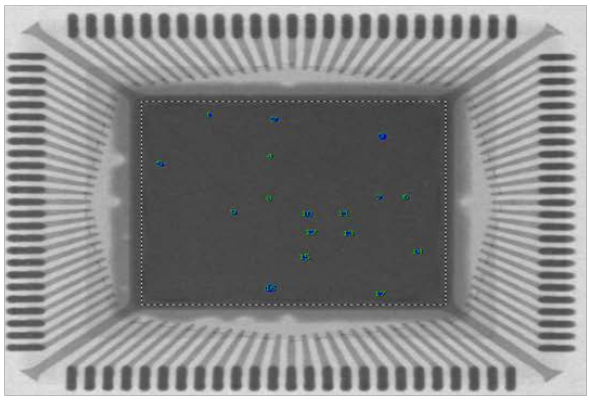

Object Count	17
Object Area	833
Total Area	1327104
Total Area Ratio	0.06%
AOI Area	148608
AOI Area Ratio	0.56%

Figure 27: Change EP. HT to OSP in 2 Images above.